Journal of
Ceramic Science
and Technology

J. Ceram. Sci. Tech., 07 [04] 433-440 (2016)
DOI: 10.4416/JCST2016-00073
available online at: http://www.ceramic-science.com

Phase Relations in the SiC-Al_2O_3-Pr_2O_3 System

W. Pan, L. Wu*, Y. Jiang, Z. Huang

School of Materials Science and Engineering, Beifang University of Nationalities, 750021 Yinchuan, China
received July 15, 2016; received in revised form September 17, 2016; accepted November 2, 2016

Abstract

Phase relations in the Si-Al-Pr-O-C system, including the SiC-Al_2O_3-Pr_2O_3, the Al_2O_3-Pr_2O_3-SiO_2 and the SiC-Al_2O_3-Pr_2O_3-SiO_2 subsystems, were determined by means of XRD phase analysis of solid-state-reacted samples fabricated by using SiC, Al_2O_3, Pr_2O_3 and SiO_2 powders as the starting materials. Subsolidus phase diagrams of the systems were presented. Two Pr-aluminates, namely $PrAlO_3$ (PrAP) and $PrAl_{11}O_{18}$ (β(Pr) β-Al_2O_3 type) were formed in the SiC-Al_2O_3-Pr_2O_3 system. SiC was compatible with both of them. Pr-silicates of Pr_2SiO_5, $Pr_2Si_2O_7$ and $Pr_{9.33}Si_6O_{26}$ (H(Pr) apatite type) were formed owing to presence of SiO_2 impurity in the SiC powder. The presence of the SiO_2 extended the ternary system of SiC-Al_2O_3-Pr_2O_3 into a quaternary system of SiC-Al_2O_3-SiO_2-Pr_2O_3 (Si-Al-Pr-O-C). SiC was compatible with Al_2O_3, Pr_2O_3 and the Pr-silicates. The effect of SiO_2 on the phase relations and liquid phase sintering of SiC ceramics was discussed.

Keywords: Pr_2O_3, SiC, phase equilibrium, solid-state reacted

I. Introduction

SiC is one of the best structural ceramics available owing to its excellent mechanical properties, creep resistance and oxidation resistance at high temperatures up to 1600 °C. However, it is difficult to densify SiC ceramics because of the strong covalence bond and the low diffusion coefficient of the SiC compound. In previous research, the Al-B-C [1–5] and the Al_2O_3-RE_2O_3 (RE-Rare Earths) systems [6–10] were used in densification of the SiC. The Al_2O_3-RE_2O_3 oxides as the liquid-phase sintering aids for the SiC ceramics lowered the sintering temperatures [11–12] and the obtained SiC ceramics exhibited relatively good mechanical properties. Although there have been many reports on the effects of the addition of Nd_2O_3, Gd_2O_3, Yb_2O_3 and Y_2O_3 on the sintering of the SiC ceramics [13–18], the addition of Pr_2O_3 as a sintering aid to the SiC ceramics has not yet been reported.

According to the Al_2O_3-Pr_2O_3 binary phase diagram [19–20], $PrAlO_3$ (PrAP) and $PrAl_{11}O_{18}$ (β(Pr), β-Al_2O_3 type) are formed based on the reactions of Al_2O_3 with Pr_2O_3. However, the lowest temperature limits for the formation of the two compounds have not yet been determined. The existence of $Pr_4Al_2O_9$ (PrAM) in the system is also disputed. This situation confused the establishment of the phase relations in Al_2O_3-Pr_2O_3-containing systems. Moreover, Refs. [21–23] reported the existence of praseodymium silicate thin films at the interfaces when polycrystalline Pr_2O_3 was deposited on SiC substrate. However, the compatibility of Pr_2O_3 and SiC at high temperature is not clear. In addition, since formation of solid solutions has been known in the SiC-Al_2O_3-RE_2O_3 (RE = Nd, Gd, Yb) systems [16–18], it is worth exploring whether similar solid solutions form in the parallel SiC-Al_2O_3-Pr_2O_3 system.

The present work investigated the phase relations in the Pr_2O_3-Al_2O_3-SiC system. With regard to the possible effect of the SiO_2 impurity in the SiC powder on the phase relations, SiO_2 was added to the system to expand the scope of research. Therefore, the phase relations in Pr_2O_3-Al_2O_3-SiC-SiO_2 quaternary system were established.

II. Experimental

(1) Materials and pretreatment

The starting powders used in the experiment were α-SiC (UF15, D_{50} = 0.6 μm, purity > 95 % with 0.5 wt% O, H.C. Starck, Germany); Al_2O_3 (D_{50} = 0.3 μm, purity > 99.99 %, Xuancheng Jingrui New Material Co., Ltd., China); Pr_6O_{11} (D_{50} = 2 – 3 μm, purity > 99.95 %, Baotou Research Institute of Rare Earths, China); SiO_2 (D_{50} = 1 μm, purity > 99.0 %, Tianjin Kemiou Chemical Reagent Co., China). Before they were used, the Al_2O_3 and the Pr_6O_{11} powders were calcined at 1200 °C for 2 h in air and in argon, respectively, to remove hydrate and to transform the Pr_6O_{11} into phase-pure Pr_2O_3. Praseodymium oxides have many valence states PrO_x (x = 1.5 – 2). While Pr_6O_{11} is the most stable state at room temperature, it releases part of the lattice oxygen at high temperatures to form Pr_2O_3 [24–25]. Oxidation of the SiC by the Pr_6O_{11} at high temperatures may take place when the Pr_6O_{11} is added to the SiC powder. To avoid the oxidation of SiC, the Pr_6O_{11} raw powder was transformed into Pr_2O_3 before the experiment.

(2) Sample preparation

Twenty-nine samples were prepared. The compositions of the samples under investigation are listed in Table 1. The

* Corresponding author: lanerwu@126.com

samples were labeled by a prefix PASS' (with each character referring to each component of Pr_2O_3, Al_2O_3, SiC and SiO_2, respectively) and a series of numbers to refer to the concentration of the components. For example, the code PASS'3151 stood for the sample with the composition of Pr_2O_3:Al_2O_3:SiC:SiO_2 = 3:1:5:1 in molar ratio, Table 1.

The starting materials were manually mixed with an agate pestle and mortar for 2 h using anhydrous ethanol as medium. After being dried, batches of the powder mixtures were uniaxially pressed in a steel mold with an inner diameter of 10 mm at 70 MPa for 30 s. Solid state reaction was performed in a furnace with graphite heating elements (Materials Research Furnaces, Inc., USA) in an Ar atmosphere at 1250 – 1750 °C for 2 – 4 h. The heating and cooling rate was 10 and 20 °C/min, respectively. Phase equilibrium was presumably achieved if no further phase changes were observed when the holding time at that temperature was prolonged.

Table 1: Compositions of the samples under investigation.

Sample code	Composition (mol.)			
	Pr_2O_3	Al_2O_3	SiC	SiO_2
PASS'0110	0	1	1	0
PASS'1010	1	0	1	0
PASS'1B00	1	11	0	0
PASS'2100	2	1	0	0
PASS'1100	1	1	0	0
PASS'1110	1	1	1	0
PASS'1BB0	1	11	11	0
PASS'5110	5	1	1	0
PASS'2110	2	1	1	0
PASS'3220	3	2	2	0
PASS'2550	2	5	5	0
PASS'0011	0	0	1	1
PASS'0302	0	3	0	2
PASS'0332	0	3	3	2
PASS'2011	2	0	1	1
PASS'90AA	9	0	10	10
PASS'70BB	7	0	11	11
PASS'2099	2	0	9	9
PASS'3101	3	1	0	1
PASS'X30X	25	3	0	25
PASS'2301	2	3	0	1
PASS'D40E	13	4	0	14
PASS'1906	1	9	0	6
PASS'1105	1	1	0	5
PASS'3151	3	1	5	1
PASS'2351	2	3	5	1
PASS'D4FE	13	4	15	14
PASS'1976	1	9	7	6
PASS'1135	1	1	3	5

*A-F in the last four characters in the codes of the samples are the hexadecimal characters representing the numbers 10 – 15, respectively. X = 25.

Table 2: XRD phase compositions of the sintered samples.

Sample code	*T* (°C)	*t* (h)	Phase composition
PASS'0110	1650	2	Al_2O_3(s); SiC(s)
PASS'1010	1650	2	Pr_2O_3(s); SiC(w)
PASS'1B00	1620	2	Al_2O_3(s); $PrAlO_3$(s); $Pr_{0.833}Al_{11.833}O_{19}$(w)
	1700	3	$Pr_{0.833}Al_{11.833}O_{19}$(s); $PrAlO_3$(m); Al_2O_3(w)
PASS'2100	1750	4	$PrAlO_3$(s); Pr_2O_3(w)
PASS'1100	1750	4	$PrAlO_3$(s)
PASS'1110	1650	2	$PrAlO_3$(s); SiC(w)
PASS'1BB0	1650	2	$PrAlO_3$(s); $Pr_{0.833}Al_{11.833}O_{19}$(s); Al_2O_3(m); SiC(m)
PASS'5110	1650	2	$PrAlO_3$(m); Pr_2O_3(s); SiC(w)
PASS'2110	1650	2	$PrAlO_3$(s); Pr_2O_3(m); SiC(w)
PASS'3220	1650	2	$PrAlO_3$(s); Pr_2O_3(m); SiC(w)
PASS'2550	1650	2	$PrAlO_3$(s); Al_2O_3(w); SiC(w); $Pr_{0.833}Al_{11.833}O_{19}$(w)
PASS'0011	1600	2	SiO_2(s); SiC(s)
PASS'0302	1600	2	Al_2O_3(s); SiO_2(m); mullite(s)
PASS'0332	1400	2	SiO_2(s); Al_2O_3(s); mullite(w); SiC(s)
PASS'2011	1400	2	Pr_2O_3(s); Pr_2SiO_5(m); SiC(vw)
PASS'90AA	1400	2	$Pr_{9.33}Si_6O_{26}$(s); SiC(w); Pr_2SiO_5(m)
PASS'70BB	1400	2	$Pr_{9.33}Si_6O_{26}$(s); $Pr_2Si_2O_7$(m); SiC(w)
PASS'2099	1400	2	$Pr_2Si_2O_7$(s); SiC(m); SiO_2(m)
PASS'3101	1400	2	$Pr_{9.33}Si_6O_{26}$(s); Pr_2O_3(s); $PrAlO_3$(s)
PASS'X30X	1400	2	Pr_2O_3(m); $Pr_{9.33}Si_6O_{26}$(s); $PrAlO_3$(w)
PASS'2301	1400	2	$PrAlO_3$(s); $Pr_2Si_2O_7$(w); Al_2O_3(w)
PASS'D40E	1400	2	$Pr_{9.33}Si_6O_{26}$(s); $Pr_2Si_2O_7$(m); $PrAlO_3$(m)
PASS'1906	1400	2	Al_2O_3(s); $Pr_2Si_2O_7$(s); mullite(m)
PASS'1105	1250	2	$Pr_2Si_2O_7$(s); SiO_2(s); mullite(m)
PASS'3151	1400	2	Pr_2O_3(s); $PrAlO_3$(s); $P_{r9.33}Si_6O_{26}$(s); SiC(w)
PASS'2351	1400	2	$PrAlO_3$(s); Al_2O_3(w); $Pr_2Si_2O_7$(m); SiC(w)
PASS'D4FE	1400	2	$Pr_{9.33}Si_6O_{26}$(s); $Pr_2Si_2O_7$(m); $PrAlO_3$(m); SiC(w)
PASS'1976	1400	2	$Pr_2Si_2O_7$(s); Al_2O_3(s); SiC(m); mullite(m)
PASS'1135	1250	2	SiO_2(s); $Pr_2Si_2O_7$(s); SiC(m); mullite(m)

* s, m, w in the brackets stood for the intensity levels of the XRD peaks. s = strong; m = middle; w = weak.

(3) Phase identification of the sintered samples

After sintering, about 0.5 – 1-mm-thick material was ground off from the surface of each sintered sample to eliminate possible contamination. Phase compositions were detected with an x-ray diffractometer (XRD-6000, Shimadzu, Japan) with Cu Kα radiation. The XRD scan was performed at a scanning rate of 4°/min with a step size of 0.02° in the 2θ range of 10 – 80°. MDI Jade 6.5 software (Materials Data Inc., USA) was used for the XRD data analysis. Phase compositions of the sintered samples indicated by XRD are shown in Table 2.

III. Results and Discussion

(1) Preparation of pure Pr_2O_3

Owing to the multicovalent states of the Pr^{n+} cations and hydration, PrO_2 and $Pr(OH)_3$ are always detected in the starting powder of Pr_6O_{11}. To avoid oxidation of SiC by Pr_6O_{11} at high temperatures, ways to prepare phase-pure Pr_2O_3 were compared by calcinating Pr_6O_{11} powder in air or in Ar at 1200 °C for 2 h. The XRD of the as-heat-treated powders are shown in Fig. 1. Phase-pure Pr_2O_3 (PDF#47 – 1111) was obtained by heating in Ar while calcination in air resulted in phase-pure Pr_6O_{11}.

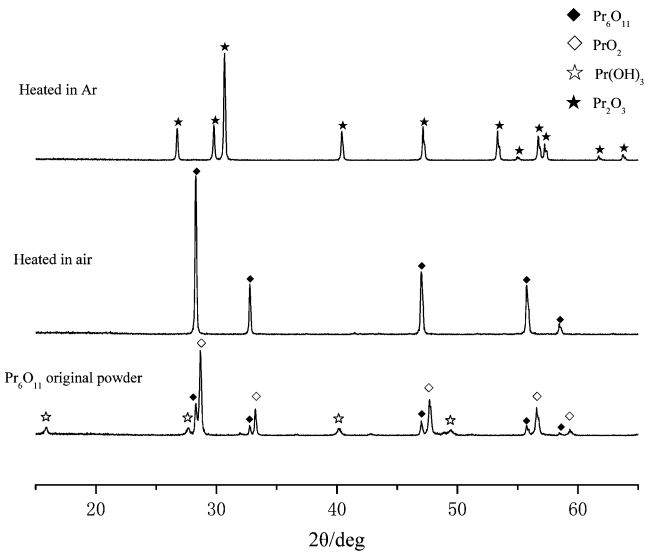

Fig. 1: XRD patterns of Pr_6O_{11} calcined at 1200 °C for 2 h in different atmospheres.

The obtained Pr_2O_3 powder was sealed and then stored in a drying vessel filled with dehydrated air. Phase changes of the powder were compared with that of the Pr_2O_3 exposed to open air. XRD analysis results of the samples are shown in Fig. 2. No noticeable change was observed in the Pr_2O_3 powder when it was sealed for 34 days or exposed for two days. But trace $Pr(OH)_3$ was detected in the powder that was exposed to air for five days. The experiments were conducted during only one day to avoid deterioration of the powder.

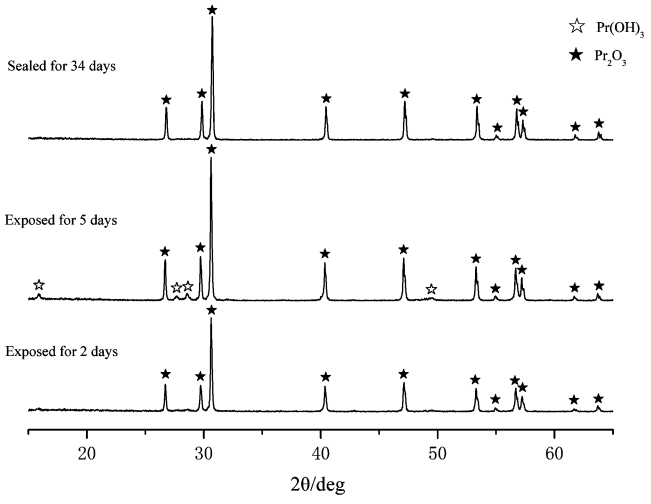

Fig. 2: XRD patterns of Pr_2O_3 stored under different conditions.

(2) Phase relations in the binary subsystems

The Si-Al-Pr-O-C system consists of six binary subsystems, namely SiC-Al_2O_3, SiC-SiO_2, SiC-Pr_2O_3, Al_2O_3-Pr_2O_3, Al_2O_3-SiO_2 and SiO_2-Pr_2O_3.

(a) *Compatibilities of SiC with the oxides*

Phase compositions of the as-sintered samples are listed in Table 2. No binary compound was detected in the PASS'0110, PASS'0011 and PASS'1010 samples (for the detailed composition of each sample, see Table 1), indicating SiC was compatible with each of the oxides of Al_2O_3, SiO_2 and Pr_2O_3 at temperatures up to 1600 °C, although reactions of $2SiO_2 + SiC \rightarrow 3SiO(g) + CO(g)$ at 1723 °C and $SiC + Al_2O_3 \rightarrow Al_2O(g) + CO(g) + SiO(g)$ at 1800 °C have been reported [26–28].

(b) *Phases in the Al_2O_3-Pr_2O_3 system*

$PrAlO_3$ was formed in the Pr_2O_3-Al_2O_3 binary system. The lowest temperature limit for the formation of the $PrAlO_3$ phase was determined at about 900 °C.

Sample PASS'2100 (Table 1) was sintered at 1750 °C for 4 h to investigate the controversial $Pr_4Al_2O_9$. No PrAM was detected. In fact, the PrAM phase was not detected in the whole temperature range of 1250 – 1750 °C, regardless of the variation of the holding times at the sintering temperatures, which is consistent with the findings of M. Mizuno [20].

Different temperatures were also tested for the sintering of the PASS'1B00 composition (Table 1) to investigate the β(Pr) phase. The XRD analysis results of the samples are shown in Fig. 3. Only $PrAlO_3$ and Al_2O_3 were detected at 1600 °C whereas the β(Pr) phase with a composition of $Pr_{0.833}Al_{11.833}O_{19}$ (PDF#82 – 0327) formed at 1620 °C and above. The concentration of the β(Pr) phase in the samples increased with the sintering temperatures up to 1700 °C. However, $Pr_{0.833}Al_{11.833}O_{19}$ was always accompanied by $PrAlO_3$ and Al_2O_3, despite regulation of the Pr_2O_3:Al_2O_3 ratios in the starting powder mixtures. In fact, the $Pr_{0.833}Al_{11.833}O_{19}$ was a solid solution of $PrAl_{11}O_{18}$ with 0.416 Al_2O_3 dissolved in it. During cooling from the high sintering temperatures, a reaction of $Pr_{0.833}Al_{11.833}O_{19} \rightarrow 0.833PrAlO_3 + 5.5Al_2O_3$ may take place, which would explain the $PrAlO_3$ and Al_2O_3 accompanied by $Pr_{0.833}Al_{11.833}O_{19}$.

(c) *Phases in the SiO_2-Al_2O_3 and the SiO_2-Pr_2O_3 systems*

Mullite was identified as the only binary compound in the Al_2O_3-SiO_2 subsystem (refer to PASS'0302 in Table 2), in agreement with N.A. Toropov [29].

There were three binary phases in the SiO_2-Pr_2O_3 subsystem, i.e. Pr_2SiO_5, $Pr_{9.33}Si_6O_{26}$ (H(Pr) apatite type) and $Pr_2Si_2O_7$, similar to that of other rare earth oxides [17–18, 30–33]. Formation of the $Pr_{9.33}Si_6O_{26}$ phase preceded the other two praseodymium silicates of Pr_2SiO_5 and $Pr_2Si_2O_7$, despite the compositions. Therefore, the formation of either Pr_2SiO_5 or $Pr_2Si_2O_7$ seemed to consist of two steps, i.e. the SiO_2 reacted with Pr_2O_3 to form $Pr_{9.33}Si_6O_{26}$ in the first step; further diffusion of the ions in the second step formed Pr_2SiO_5 or $Pr_2Si_2O_7$ according to the composition in equilibrium.

(3) Phase relations in the ternary subsystems

The Si-Al-Pr-O-C system consists of four ternary subsystems, i.e. Pr_2O_3-Al_2O_3-SiC, SiC-SiO_2-Pr_2O_3, SiC-SiO_2-Al_2O_3 and Pr_2O_3-Al_2O_3-SiO_2.

(a) *Phases in the SiC-Al_2O_3-SiO_2 system*

Mullite was the only phase in the Al_2O_3-SiO_2 system. The phase compositions (Table 2) in the as-sintered sample of PASS'0332 showed compatibility of SiC with mullite, in accordance with Refs. [16–17].

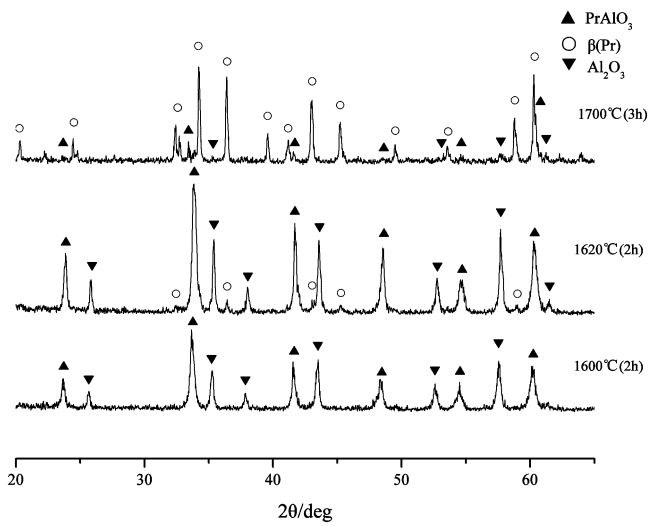

Fig. 3: XRD patterns of PASS'1B00 in different temperatures.

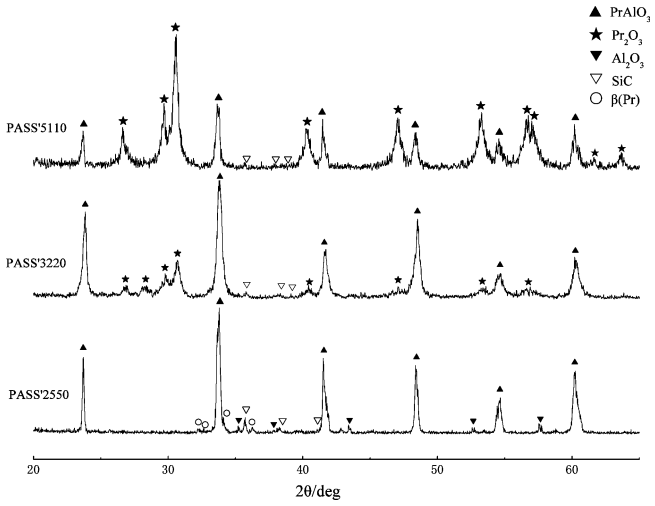

Fig. 5: XRD patterns of PASS'5110, PASS'3220 and PASS'2550 after sintering at 1650 °C for 2 h.

(b) *Phases in the Pr_2O_3-Al_2O_3-SiC system*

A tentative phase diagram of the Pr_2O_3-Al_2O_3-SiC ternary system is shown in Fig. 4. The compositions marked by the dots were chosen to check the phase relations in the system. The respective compositions of the numbers beside the dots refer to Table 1. Selected XRD patterns of the as-sintered samples of PASS'5110, PASS'3220 and PASS'2550 are shown in Fig. 5. The phase compositions of all the samples are listed in Table 2.

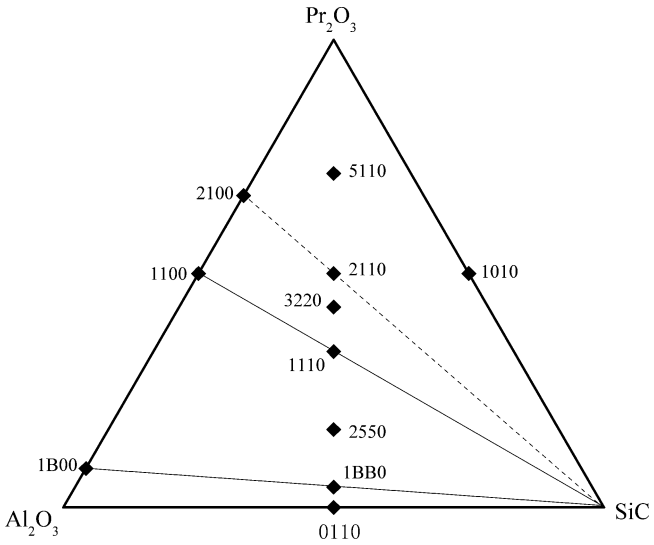

Fig. 4: The points investigated in the tentative Pr_2O_3-Al_2O_3-SiC system.

The addition of SiC had no effects on the formation of the PrAP and the β(Pr) phase. The PrAP and the β(Pr) were the only binary compound formed in the system. Coexistence of SiC with each of the PrAP and the β(Pr) phases was demonstrated. Therefore, the SiC-PrAP and the SiC-β(Pr) tie-lines were proved in the phase relations of the Pr_2O_3-Al_2O_3-SiC system, as shown in Fig. 6. Because there was no compound with a chemistry of $2Pr_2O_3 \cdot Al_2O_3$ formed, the proposed SiC-$Pr_4Al_2O_9$ tie-line in the tentative phase diagram Fig. 4 was eliminated.

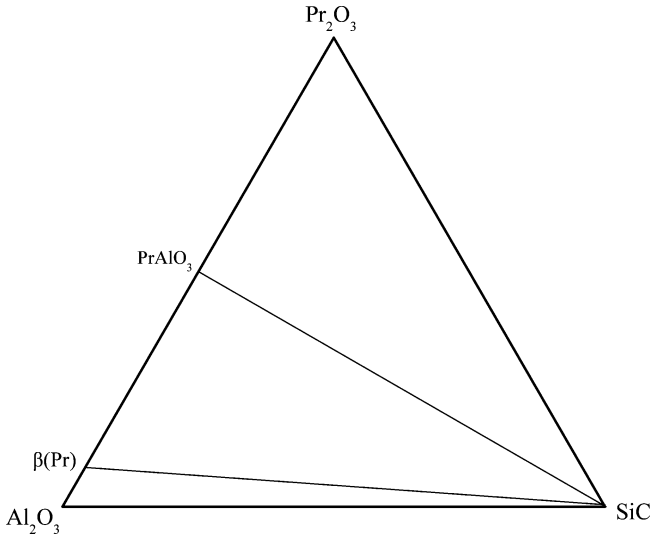

Fig. 6: Subsolidus phase diagram of the Pr_2O_3-Al_2O_3-SiC system.

(c) *Phases in the SiC-SiO_2-Pr_2O_3 system*

The phase compositions in the as-sintered samples of PASS'2011, PASS'90AA, PASS'70BB and PASS'2099 (Table 1) illustrated the phase relations in the SiC-SiO_2-Pr_2O_3 system. Three primary phases of H(Pr), Pr_2SiO_5 and $Pr_2Si_2O_7$ were formed. SiC was compatible with each of them. The presence of SiC did not affect the formation of the primary phases.

(d) *Phases in the Pr_2O_3-Al_2O_3-SiO_2 system*

According to Refs. [18, 34–35], possible phase relations in the Pr_2O_3-Al_2O_3-SiO_2 system were constructed as shown in Fig. 7. Six points as marked by the dots were selected to test the validity of the phase relations.

Selected XRD patterns of the PASS'X30X and PASS'3101 samples are shown in Fig. 8. The phase compositions of both samples are listed in Table 2. Only PrAlO$_3$ and $Pr_{9.33}Si_6O_{26}$ were revealed in the PASS'X30X sample. No Pr_2SiO_5 was discovered in either sample, indicating Pr_2SiO_5 phase did not form when Al_2O_3 was added, the same as that observed in the Nd_2O_3-Al_2O_3-SiO_2 system, owing to the formation of Al-apatite sol-

id solution [18]. Co-existence of $PrAlO_3$ and $Pr_2Si_2O_7$ could be inferred from the XRD patterns of the samples PASS'2301 and PASS'D40E, see Fig. 9 and Table 2.

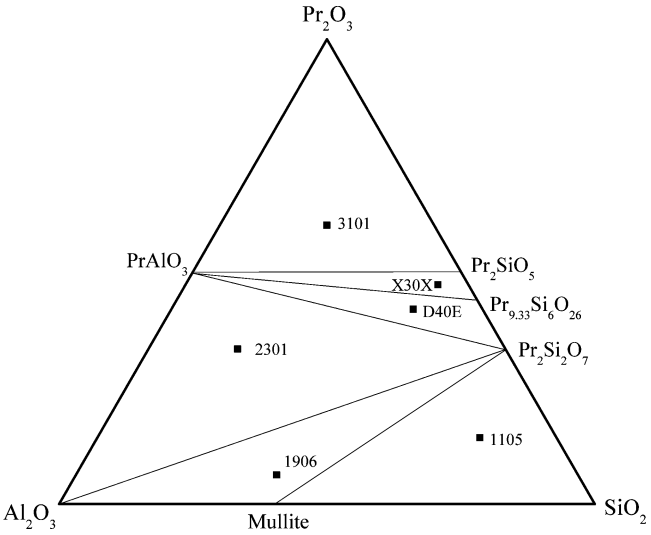

Fig. 7: The points investigated in the tentative Pr_2O_3-Al_2O_3-SiO_2 system.

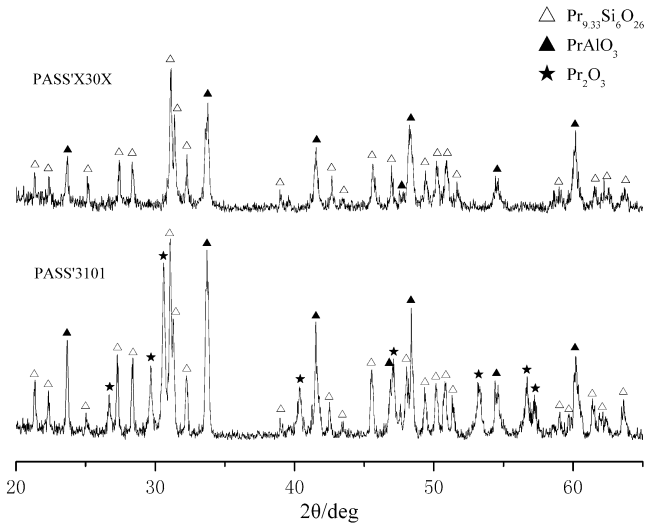

Fig. 8: XRD patterns of PASS'X30X and PASS'3101 after sintering at 1400 °C for 2 h.

The β(Pr) phase did not form at 1600 °C. However, the β(Pr) phase dominated the phase compositions when the sample PASS'1B00 was obtained by sintering at 1700 °C for 2 h and then annealed at 1400 °C for 3 h. Its XRD patterns before and after annealing are compared in Fig. 10, indicating the persistence of the β(Pr) phase. Besides, trace β(Pr) was also found in the sample PASS'2301 when this was sintered at 1650 °C for 2 h. Therefore, six three-phase coexistence triangles were formed at 1400 °C in the Pr_2O_3-Al_2O_3-SiO_2 system, i.e. $PrAlO_3$-$Pr_{9.33}Si_6O_{26}$-$Pr_2Si_2O_7$, $Pr_2Si_2O_7$-Al_2O_3-$Al_6Si_2O_{13}$, $Pr_2Si_2O_7$-$Al_6Si_2O_{13}$-SiO_2 β(Pr)-Al_2O_3-$Pr_2Si_2O_7$, $PrAlO_3$-$Pr_2Si_2O_7$-β(Pr), Pr_2O_3-$PrAlO_3$-$Pr_{9.33}Si_6O_{26}$. Accordingly, the phase relations of the ternary Pr_2O_3-Al_2O_3-SiO_2 system were established, as shown in Fig. 11.

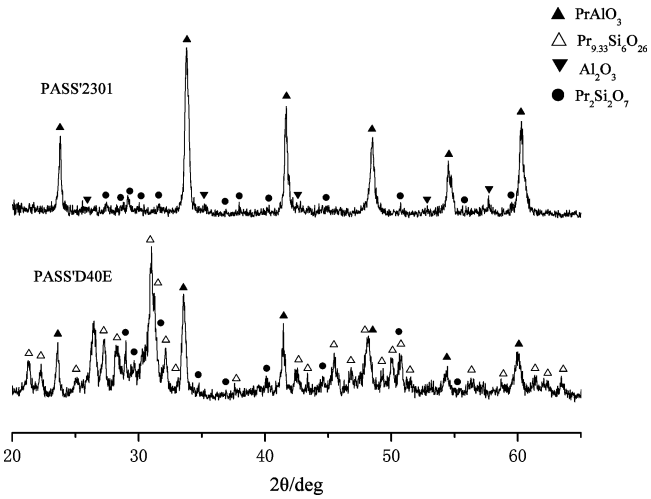

Fig. 9: XRD patterns of PASS'2301 and PASS'D40E after sintering at 1400 °C for 2 h.

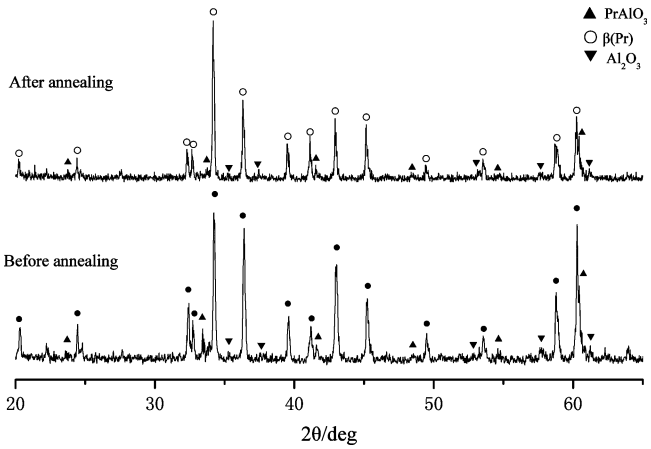

Fig. 10 : XRD patterns of PASS'1B00 before and after annealing.

(4) Phase relations in the quaternary system

Because SiO_2 was always present as an impurity in the SiC powder, the effects of the SiO_2 should be taken into account when the phase diagram is constructed. Therefore, the ternary systems were extended into a quaternary system of SiC-Al_2O_3-Pr_2O_3-SiO_2. In addition, a subsolidus phase diagram of the SiC-Al_2O_3-Pr_2O_3-SiO_2 system could only be established at lowered temperatures, such as 1400 °C, for the lower eutectic temperature of the Pr_2O_3-Al_2O_3-SiO_2 system.

The compositions used for investigation of the quaternary system were the PASS'3151, PASS'2351, PASS'D4FE, PASS'1976 and the PASS'1135 (Table 1). As an example, XRD patterns of the samples of PASS'3151 and PASS'D4FE are shown in Fig. 12. The XRD analysis results are listed in Table 2. Because SiC was compatible with each of the phases in the Al_2O_3-Pr_2O_3-SiO_2 ternary oxide system, six four-phase coexistence regions were verified, i.e. SiC-Al_2O_3-$Pr_2Si_2O_7$-β(Pr), SiC-$PrAlO_3$-$Pr_{9.33}Si_6O_{26}$-$Pr_2Si_2O_7$, SiC-Al_2O_3-$Al_6Si_2O_{13}$-$Pr_2Si_2O_7$, SiC-$PrAlO_3$-$Pr_2Si_2O_7$-β(Pr), SiC-$Pr_2Si_2O_7$-$Al_6Si_2O_{13}$-SiO_2 and SiC-Pr_2O_3-$PrAlO_3$-$Pr_{9.33}Si_6O_{26}$.

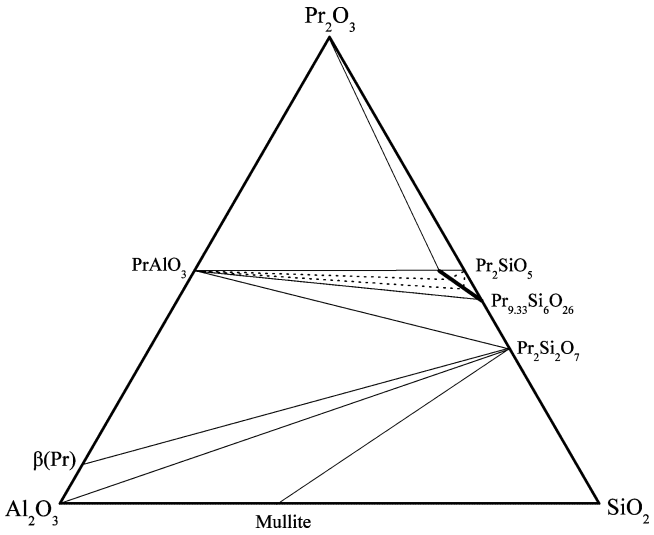

Fig. 11: Subsolidus phase diagram of the Pr_2O_3-Al_2O_3-SiO_2 system.

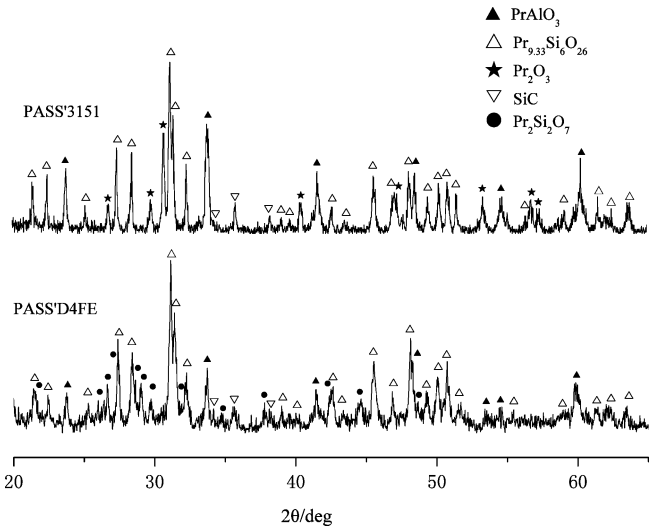

Fig. 12: XRD patterns of PASS'3151 and PASS'D4FE after sintering at 1400 °C for 2 h.

Summarizing the investigation results, the subsolidus phase diagram of the Pr_2O_3-Al_2O_3-SiO_2-SiC quaternary system was established, as shown in Fig. 13.

Before we conclude, possible effects of SiO_2 on the sintering of the SiC ceramics are briefly discussed in the following. Sample PASS'1135 contained more SiO_2 than PASS'3151 (see Table 1), XRD patterns of PASS'1135 showed a much higher background than those of PASS'3151, indicating formation of more eutectic liquid in the SiO_2-rich sample. Therefore, if SiO_2 is present when a powder mixture of Pr_2O_3-Al_2O_3 is used as the sintering aid and added to the SiC ceramics, a decrease in high-temperature properties of the consolidated SiC ceramics can be reasonably expected, although the presence of the SiO_2 lowers the sintering temperature of the SiC ceramics. The small concentrations of the oxygen in the commercially available SiC powders have to be considered carefully in the process of designing the compositions and the sintering conditions for the manufacture of the SiC ceramics.

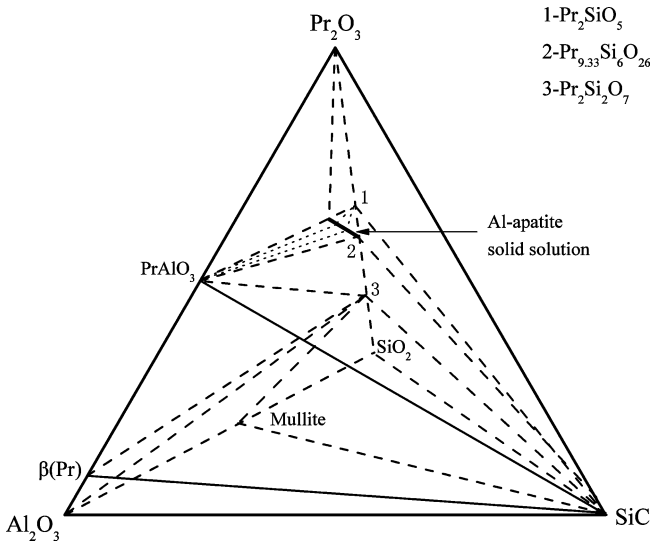

Fig. 13: Subsolidus phase diagram of the SiC-Pr_2O_3-Al_2O_3-SiO_2 system.

IV. Conclusions

(1) The existence of $PrAlO_3$ and $Pr_{0.833}Al_{11.833}O_{19}$ was verified in SiC-Al_2O_3-Pr_2O_3 ternary system, and both were able to coexist with SiC, while the controversial $Pr_4Al_2O_9$ was never found. The subsolidus phase diagram of the Al_2O_3-SiC-Pr_2O_3 ternary system was presented.

(2) SiC was compatible with Pr_2SiO_5, $Pr_{9.33}Si_6O_{26}$ and $Pr_2Si_2O_7$ respectively in the SiO_2-SiC-Pr_2O_3 ternary system. However, when Al_2O_3 is added, the formation of Al-apatite solid solution will result in Pr_2SiO_5 disappearing.

(3) The subsolidus phase diagram of the Pr_2O_3-Al_2O_3-SiC-SiO_2 quaternary system containing six four-phase compatibility tetrahedra was established at 1400 °C.

(4) Pr_2O_3-Al_2O_3 may be suitable as a sintering aid for the manufacture of the SiC ceramics despite the SiO_2 impurity in the SiC powder. But a higher concentration of SiO_2 would reduce the mechanical properties of the consolidated SiC ceramics at high temperatures.

Acknowledgement

The present work was financially supported by National Natural Science Foundation of China, under grant numbers of NSFC51362001.

References

1 Biswas, K.: Solid state sintering of SiC-ceramics, *Mater. Sci. Forum*, **624**, 71 – 89, (2009).

2 Bocker, W., Landfermann, H., Hausner, H.: Sintering of alpha silicon carbide with additions of aluminum, *Powder Metall. Int.*, **11**, [2], 83 – 85, (1979).

3 Wu, A.H., Cao. W.B., Li. J.T., Ge, C.C.: Solid state sintered SiC ceramics, *J. Mater. Eng.*, [4], 3 – 5, (2001).

4 Wu, A.H., Cao. W.B., Li. J.T., Ge, C.C.: Progress in SiC sintering, *Powder Metal. Ind.*, **12**, [3], 28 – 32, (2002).

5 Alligeo, R.A., Coffin, L.B., Tinklpaugh, J.R.: Pressure-sintered silicon carbide, *J. Am. Ceram. Soc.*, **39**, [11], 386 – 389, (1956).

6 Omori, M., Takei, H.: Pressureless sintering of SiC, *J. Am. Ceram. Soc.*, **65**, [6], c92 – c92, (1982).

7 Tan, S.H., Chen, Z.M, Jiang, D.L.: Liquid phase sintered SiC ceramics, *J. Chin. Ceram. Soc.*, **26**, [2], 191 – 197, (1998).

[8] Zhou, W., Cai, Z.H., Zeng, J., Chen, X.J., Huang, Q.J., Lan, L., Chen, L.F.: Effects of sintering additives on the liquid-phase sintering of SiC, *J. Xiamen University (Natural Science)*, **45**, [4], 530 – 534, (2006).

[9] Chang, Y.W.: Research on preparation of high performance SiC ceramic materials, *Nanjing University of Science and Technology (master thesis)*, 21 – 26, (2009).

[10] Hu, J.L., Hu, C.Y., Liu, X., Tian, X.Y.: Research progress on preparation methods of SiC powder and its sintering aids, *Bull. Chin. Ceram. Soc.*, **33**, [9], 2280 – 2284, (2014).

[11] Wu, A.H., Cao. W.B., Li. J.T., Ge, C.C.: Microstructure study on liquid phase sintered SiC, *Bull. Chin. Ceram. Soc.*, **20**, [2], 55 – 58, (2001).

[12] Wu, L.E., Chen, Y.H., Jiang , Y., Huang, Z.K.: Liquid phase sintering of SiC with AlN-RE_2O_3 additives, *J. Chin. Ceram. Soc.*, **36**, [5], 593 – 596, (2008).

[13] Omori, M., Takei, H.: Preparation of pressureless-sintered SiC-Y_2O_3-Al_2O_3, *J. Mater. Sci.*, **23**, [10], 3744 – 3749, (1988).

[14] Wu, K., Wu, L.E., Huang, Z.K., Jiang, Y., Ma, Y.: Phase relations in Si-Al-Y-O-C systems, *J. Mater. Sci. Chem. Eng.*, **03**, [7], 90 – 96, (2015).

[15] Jiang, Y., Wu, L.E., Wei, Z.B., Huang, Z.K.: Phase relations in the SiC-Al_2O_3-Y_2O_3 system, *Mater. Lett.*, **165**, 26 – 28, (2015).

[16] Wei, Z.B., Jiang, Y., Liu, L.M., Wu, L.E., Huang, Z.K.: Phase relations in the Si-Al-Yb-O-C system, *J. Eur. Ceram. Soc.*, **36**, [3], 437 – 441, (2016).

[17] Wei, Z.B., Jiang, Y., Liu, L.M., Wu, L.E., Huang, Z.K.: Phase relations in the Si-Al-Gd-O-C system, *Ceram. Int.*, **42**, [2], 2605 – 2610, (2016).

[18] Ma, Y., Wu, L.E., Huang, Z.K., Jiang, Y., Liu, L.M.: Phase relations in Si-Al-Nd-O-C system, *J. Phase Equilib. Diff.*, **37**, [5], 532 – 539, (2016).

[19] Wu, P., Pelton, A.D.: Coupled thermodynamic-phase diagram assessment of the rare earth oxide-aluminium oxide binary systems, *J. Alloy. Compd.*, **179**, 259 – 287, (1992).

[20] Mizuno, M., Yamada, T., Noguchi, T.: Phase diagram of the system Al_2O_3-Pr_2O_3 at high temperature, *J. Ceram. Soc. Jpn.*, **85**, [1], 24 – 29, (1977).

[21] Goryachko, A., Paloumpa, I., Beuckert, G., Burkov, Y., Schmeisser, D.: The interaction of Pr_2O_3 with 4H-SiC(0001) surface, *Phys. Stat. Sol. (C)*, **1**, [2], 265 – 268, (2004).

[22] Nigro, R.L., Toro, R.G., Malandrino, G., Fragalà, I.L., Raineri, V., Fiorenza, P.: Praseodymium based high-k dielectrics grown on si and SiC substrates, *Mat. Sci. Semicon. Proc.*, **9**, [6], 1073 – 1078, (2006).

[23] Sohal, R., Torche, M., Henkel, K., Hoffmann, P., Tallarida, M., Schmeisser, D.: Al-oxynitrides as a buffer layer for Pr_2O_3/SiC interfaces, *Mat. Sci. Semicon. Proc.*, **9**, [6], 945 – 948, (2006).

[24] Peng, S.J.: Microstructural and nonlinear electrical property of prraseodymium trioxide ceramic, *Southwest Jiaotong University(master thesis)*, 18 – 20, 2013.

[25] Ying, P.L., Li, C., Xin, Q.: Desorption and reactivity of lattice oxygen species in praseodymium oxide studied by TPD-MASS spectroscopy, *J. Catal.*, **14**, [6], 488 – 492, (1993).

[26] Borisov, V.G., Yudin, B.F.: Reaction thermodynamics in the SiO_2-SiC system, *Refractories*, *USSR*, **9**, 162 – 165, (1968).

[27] Gadalla, A., Elmasry, M., Kongkachuichay, P.: High temperature reactions within SiC-Al_2O_3 composites, *J. Mater. Res.*, **7**, [9], 2585 – 2592, (1992).

[28] Mulla, M.A., Krstic, V.D., Thompson, W.T.: Reaction-inhibition during sintering of SiC with Al_2O_3 additions, *Canad. Metall. Quarter.*, **34**, [4], 357 – 362, (1995).

[29] Toropov, N.A., Galakhov, F.I.: Solid solutions in the system Al_2O_3-SiO_2, *Bull. Acad. Sci. USSR*, **7**, [1], 5 – 9, (1958).

[30] Toropov, N.A., Bondar, I.A.: Silicates of the rare earth elements: phase diagram of the binary system yttrium oxide-silica, *Bull. Acad. Sci. USSR, Div. Chem. Sci.*, **10**, [4], 502 – 508, (1961).

[31] Toropov, N.A., Bondar, I.A., Galakhov, F.Y.: High-temperature solid solutions of silicates of the rare earth elements, *Trans. Int. Ceram. Congr., 8th, Copenhagen*, 85 – 103, (1962).

[32] Toropov, N.A., Bondar, I. A.: Silicates of the rare earth elements, *Bull. Acad. Sci. USSR*, **10**, [8], 1278 – 1285, (1961).

[33] Toropov, N.A.: Some rare earth silicates, *Trans. Int. Ceram. Congr., 7th, London*, 435 – 442, (1960).

[34] Kaiser, A., Telle, R., Herrmann, M., Richter, H.J., Hermel, W.: Subsolidus phase relationships of the ß-sialon solid solution in the oxygen-rich part of the Nd-Si-Al-O-N system, *Int. J. Mater. Res.*, **92**, [10], 1163 – 1169, (2001).

[35] Kaiser, M., Richter, H.J., Herrmann, M., Hermel, W.: Subsolidus phase relationships in the Nd-Si-Al-O-N system, *Key Eng. Mat.*, **1**, [1], 369 – 372, (1993).